

# Mechanism of the Photocatalytic Oxidation of Ethanol on TiO<sub>2</sub>

Darrin S. Muggli, Justin T. McCue, and John L. Falconer<sup>1</sup>

*Department of Chemical Engineering, University of Colorado, Boulder, Colorado 80309-0424*

Received July 11, 1997; revised October 17, 1997; accepted October 22, 1997

Transient, isothermal photocatalytic oxidation (PCO) was combined with isotope labeling and temperature-programmed desorption and oxidation to directly identify reaction pathways and intermediates for the room-temperature PCO of ethanol on TiO<sub>2</sub>. The intermediates identified are acetaldehyde, acetic acid (acetate), formaldehyde, and formic acid (formate). The  $\alpha$ -carbons of ethanol, acetaldehyde, and acetic acid were labeled with <sup>13</sup>C so that the reaction pathway of each carbon could be followed. For each molecule, the  $\alpha$ -carbon preferentially oxidized to CO<sub>2</sub> as the two-carbon species were sequentially oxidized. Ethanol forms acetaldehyde, which either desorbs or oxidizes through at least two parallel pathways, only one of which involves acetic acid. Part of the ethanol reacts on the surface through the pathway: acetaldehyde  $\rightarrow$  acetic acid  $\rightarrow$  CO<sub>2</sub> + formaldehyde  $\rightarrow$  formic acid  $\rightarrow$  CO<sub>2</sub>. The remaining ethanol oxidizes more slowly through a pathway that does not contain acetic acid as an intermediate: acetaldehyde  $\rightarrow$  formic acid + formaldehyde  $\rightarrow$  formic acid  $\rightarrow$  CO<sub>2</sub>. The oxidation of ethanol to acetaldehyde is not the rate-determining step. The oxidations of formaldehyde to formic acid, and formic acid to CO<sub>2</sub>, occur at about the same rate, which is faster than acetic acid oxidation. Acetaldehyde oxidizes to form intermediates at approximately the same rate as they are oxidized. The presence of acetaldehyde on the surface, however, decreases the reactivity of other intermediates, suggesting that increasing the rate of acetaldehyde oxidation would increase the overall rate of CO<sub>2</sub> production.

© 1998 Academic Press

## INTRODUCTION

Heterogeneous photocatalytic oxidation (PCO) has potential applications for the complete oxidation of organic pollutants in dilute systems. Organics can be oxidized to CO<sub>2</sub> and H<sub>2</sub>O at room temperature on TiO<sub>2</sub> catalysts in the presence of UV or near-UV illumination. The UV light excites electrons from the valence to the conduction band of the semiconductor catalyst, leaving holes behind. The electron-hole pairs can initiate redox reactions with surface species. Although recent studies have shown that PCO can oxidize a number of gas-phase organic compounds (1–12), the reaction mechanisms are poorly understood and the in-

termediates, particularly if they do not leave the catalyst, are often not identified. Oxidation of aqueous phase organics has been studied more extensively, but the mechanism may be quite different for the gas phase reactants.

In this study, ethanol was used as a model reactant to elucidate the mechanism of PCO on TiO<sub>2</sub>. Ethanol oxidation is of interest because it is a pollutant from industrial processes such as breweries and bakeries. Previously, we have shown that the  $\alpha$ -carbon in ethanol is preferentially oxidized to CO<sub>2</sub> (1) and hypothesized that ethanol reacts through at least two parallel pathways. In our current work, the reaction intermediates, some of which do not desorb from the catalyst during PCO, are identified and a mechanism that includes two parallel reaction pathways is proposed.

Transient techniques are especially useful for studying photocatalytic oxidation. The buildup and consumption of intermediates on the catalyst surface can be followed by turning off the UV lights after various reaction times (to stop PCO) and performing temperature-programmed desorption (TPD). An added advantage of these transient reaction experiments is that only a monolayer or submonolayer of organic is reacted, and thus the surface species detected during TPD are more likely to be intermediates and not spectator species accumulating on the surface from a side reaction. Transient reaction techniques allow the separation of adsorption, surface reaction, and desorption steps. Adsorption was isolated from the other steps by exposing the catalyst to an organic vapor at room temperature in the absence of UV radiation and then photocatalytically oxidizing it in an O<sub>2</sub>/He stream in the absence of the gas-phase organic. After PCO for a specified amount of time, TPD was performed to quantitatively identify intermediates that remained on the catalyst surface. Because not all products desorbed during TPD, temperature-programmed oxidation (TPO) was sometimes employed after PCO to obtain mass balances. A combination of transient isothermal PCO followed by TPO was shown recently to be useful for studying PCO of 2-propanol (13) and ethanol (1) on TiO<sub>2</sub>. A low O<sub>2</sub> concentration (0.2% O<sub>2</sub> in He) was used during PCO to decrease the reaction rate so that intermediate products were more readily detected, but the same behavior was seen in 20% O<sub>2</sub>. Water was not added to the O<sub>2</sub>/He gas stream

<sup>1</sup> E-mail: john.falconer@colorado.edu.

so that the effect of water could be determined in future studies. Moreover, for transient PCO, water would displace the weakly adsorbed ethanol if water but not ethanol were present in the gas stream. In addition, water forms during reaction and remains adsorbed on the surface, so that water was present during much of the PCO. Preliminary experiments indicate that the mechanism is similar when water is coadsorbed with ethanol.

Isotopically labeled ethanol (CH<sub>3</sub><sup>13</sup>CH<sub>2</sub>OH), acetaldehyde (CH<sub>3</sub><sup>13</sup>CHO), and acetic acid (CH<sub>3</sub><sup>13</sup>COOH) were used with the  $\alpha$ -carbons labeled with <sup>13</sup>C. By having the two carbons labeled with different carbon isotopes, we are able to follow differences in their reactivities. In addition, comparing the relative amounts of <sup>12</sup>C and <sup>13</sup>C-containing species on the catalyst after PCO was instrumental in identifying a second reaction pathway.

Photocatalytic oxidation of alcohols has been studied previously, mostly in steady state or batch reactors with the alcohol in the gas phase. Djeghri and Teichner (14) proposed parallel pathways for PCO of 3-methyl-1-butanol. They stated that alcohols typically react by both direct oxidation and dehydration. However, since the dehydration of primary alcohols is difficult, they proposed a branching, direct-oxidation mechanism to explain the appearance of the partial oxidation products: 3-methylbutanal, 2-methylpropanal, and acetone. Their mechanism did not account for the possible oxidation of 3-methylbutanal to 2-methylpropanal and acetone.

Blake and Griffin (15) also proposed two parallel pathways for the gas-phase PCO of 1-butanol on TiO<sub>2</sub>. They observed 1-butanal and 1-butene with selectivities of 89 and 11%, respectively. Although their reactions were performed with a 100-W Hg lamp in 22% O<sub>2</sub>, the feed contained 1% butanol and CO<sub>2</sub> was not observed. In addition, varying the oxygen concentration from 2 to 22% had no effect on the rate or selectivity of the reaction. However, the addition of 1% 1-butanol in the gas stream inhibited the reaction. Infrared spectra indicated the presence of butanoic acid, which was concluded to be a secondary oxidation product of 1-butanol. The butanoic acid was not detected in the gas phase during PCO, and IR studies showed that it only slowly disappeared from the surface during illumination.

Cunningham *et al.* (16) photocatalytically oxidized primary, secondary, and tertiary alcohol vapors on TiO<sub>2</sub> in the presence of oxygen (20–80%). The primary alcohol, 3-methyl-1-butanol, mainly dehydrogenated to 3-methylbutanal via  $\alpha$ -H elimination. The appearance of other products, 2-methylpropanal, ethanal, and acetone, was attributed to the subsequent oxidation of 3-methylbutanal. Similarly, 3-methyl-2-butanol mainly dehydrogenated to 3-methyl-2-butanone but also formed products via C–C bond scission at the  $\alpha$  and  $\beta$  positions. However, 3-methyl-2-butanone did not further oxidize to an appreciable ex-

tent. Because an  $\alpha$ -hydrogen is not available in the tertiary alcohol (2-methyl-2-butanol), the main products (acetone, ethanal, and 2-butanone) resulted from  $\alpha$  and  $\beta$  carbon-carbon bond scission. No alkenes were detected during PCO of the alcohols studied.

Two recent studies (17, 18) have looked at the gas-phase PCO of ethanol in batch reactors. Nimlos *et al.* (17) used a recirculating batch reactor, and identified acetaldehyde, acetic acid, formaldehyde, and formic acid as important intermediates. The gas phase concentration of formaldehyde reached a maximum after approximately 7 s of illumination with a shoulder at 1 to 4 s, suggesting two pathways leading to the formation of formaldehyde and CO<sub>2</sub>. Nimlos *et al.* also studied PCO of the intermediates. Acetaldehyde produced mainly formaldehyde and CO<sub>2</sub>, with small amounts of acetic acid, and acetic acid also formed both formaldehyde and CO<sub>2</sub> in the gas phase. The PCO of formaldehyde produced CO<sub>2</sub>, but its evolution rate was slower than the formaldehyde uptake, suggesting an intermediate, which they conjectured was formic acid. Further, FTIR studies indicated the presence of formic acid during PCO of formaldehyde.

Sauer and Ollis (18) also used a recirculating batch reactor system to study PCO of ethanol in humidified air. Two types of reactors were used: a fully illuminated glass frit reactor and a monolith reactor that had dark spots because only 3.5% of the reactor was illuminated. For the fully illuminated reactor, they proposed that ethanol reacts to acetaldehyde, which then forms CO<sub>2</sub> both directly and through a formaldehyde intermediate. However, this mechanism was not adequate to provide closure on the carbon mass balance for the monolith reactor. They proposed that acetic acid and formic acid desorbed from the illuminated portions of the catalyst and reversibly collected on the dark TiO<sub>2</sub>, but they did not directly identify these species. These species then readsorb onto the illuminated TiO<sub>2</sub> where they eventually oxidize to CO<sub>2</sub>. The authors stated that acetic acid and formic acid react quickly on illuminated TiO<sub>2</sub> and therefore are present only in low concentrations so they are not important for the fully illuminated reactor. In addition, they reported two maxima in the rate of formation of formaldehyde with time, which they attributed to acetic acid and acetaldehyde.

Both of these studies of ethanol PCO used recirculation batch reactors. Since only products that desorb during PCO were detected, some strongly bound intermediates may have been missed. Also, the probability of detecting products from minor side reactions increases with the amount of ethanol reacted. In our study, TPD after various PCO times of a monolayer of organic allows the detection of strongly bound intermediates and the changes in surface composition to be monitored. Since only a monolayer or submonolayer is reacted, the products are more likely intermediates and not from side reactions. In addition,

isotopic labeling adds more information because the reactivity of each carbon atom is monitored.

## EXPERIMENTAL METHODS

The apparatus used for PCO, TPD, and TPO was described previously (13). Degussa P-25 TiO<sub>2</sub> powder was coated as a thin layer (average thickness <0.5 μm) on the inside of an annular Pyrex reactor so that essentially all the TiO<sub>2</sub> was exposed to UV light for PCO. For a reactor with a 1-mm annular spacing, high gas flow rates could be maintained across the catalyst so as to minimize mass transfer effects and rapidly flush gas-phase products from the reactor. The outside diameter of the reactor was 2 cm and the reactor was 13 cm high so that sufficient catalyst mass was present to allow detection of reaction products by the mass spectrometer. The photocatalytic reactor was surrounded by a quartz furnace with heating wires for TPD, and the furnace was surrounded by six UV black light lamps (GE, 4 W). The light intensity at the catalyst surface, measured with a radiometer, was approximately 0.3 mW/cm<sup>2</sup>. The maximum light intensity was near 356 nm (17). The tip of a chromel-alumel thermocouple (0.5-mm diameter) contacted the side of the reactor wall to record temperature during TPD and to provide feedback to the temperature programmer.

Before each experiment, the reactor was heated in approximately 3% O<sub>2</sub> in He to 723 K in order to create a reproducible surface and then cooled to room temperature. The organic of interest was injected immediately upstream of the reactor and allowed to evaporate and adsorb onto the catalyst surface at room temperature in 0.2% O<sub>2</sub> flow. Photocatalytic oxidation and temperature-programmed desorption were performed for ethanol (Midwest Grain, 200 proof), ethyl-1-<sup>13</sup>C alcohol (CH<sub>3</sub><sup>13</sup>CH<sub>2</sub>OH, Isotec, 99+%), acetaldehyde (Aldrich, 99.5+%), acetic acid (Aldrich, 99.99+%), 1-<sup>13</sup>C acetic acid (CH<sub>3</sub><sup>13</sup>COOH, Isotec, 99+%), formic acid (Sigma, 99%), and formaldehyde (produced by heating paraformaldehyde to 400 K). All PCOs were carried out at room temperature in 0.2% O<sub>2</sub> after any excess organic was flushed from the gas phase. Experiments were performed at both saturation and partial coverages. During saturation-coverage PCO, some intermediates desorbed and were detected in the gas phase. Less-than-saturation coverage was used so that intermediates remained on the catalyst surface and their cracking fractions did not interfere with detection of <sup>12</sup>CO<sub>2</sub> and <sup>13</sup>CO<sub>2</sub>. Less than saturation coverages were used for formaldehyde because of the difficulty in obtaining larger quantities of formaldehyde from heating paraformaldehyde.

Due to the high cost of isotopically labeled acetaldehyde (CH<sub>3</sub><sup>13</sup>CHO), this isotope was produced photocatalytically. A monolayer of <sup>13</sup>C-ethanol was reacted on a second reactor located upstream, producing <sup>13</sup>C-acetaldehyde,

<sup>13</sup>CO<sub>2</sub>, <sup>12</sup>CO<sub>2</sub>, and a small amount of <sup>13</sup>C-ethanol in the gas phase. The <sup>13</sup>C-acetaldehyde and <sup>13</sup>C-ethanol adsorbed on the downstream reactor. This procedure was repeated until the desired coverage was obtained. Temperature-programmed desorption experiments indicated that the ratio of <sup>13</sup>C-acetaldehyde to <sup>13</sup>C-ethanol adsorbed on the downstream reactor was approximately 10:1.

For PCO, metal shields were placed between the reactor and the UV lights before the lights were switched on. When the lights reached a steady-state output, reaction was initiated by removing the shields. After PCO at room temperature for a time period on the order of tens of minutes, TPD was carried out by heating the catalyst in He at a constant rate of 1 K/s to 723 K. The catalyst was held at this temperature until no desorption products were detected in the gas phase. The same procedure was used to measure TPD of the organics in the absence of PCO. For some experiments, TPO was performed after PCO and TPD by heating the catalyst at the same rate in 0.2% O<sub>2</sub> flow. A Balzers QMA 125 quadrupole mass spectrometer monitored the reactor effluent immediately downstream of the reactor. The mass spectrometer was interfaced to a computer so that multiple mass peaks could be recorded simultaneously during PCO and TPD. The mass spectrometer signals were frequently calibrated by injecting known volumes of gases or liquids into the flow stream downstream of the reactor, and signals were corrected for cracking in the mass spectrometer. Calibration of the <sup>13</sup>C species was accomplished by injecting the corresponding <sup>12</sup>C species into the mass spectrometer. Although water is a reaction product, its signal is not plotted in the figures because its calibration is less accurate and because water appearance in the gas phase is limited by desorption from the TiO<sub>2</sub> surface so that the water signal does not provide kinetic information.

## RESULTS

### *Temperature-Programmed Oxidation and Desorption*

Temperature-programmed oxidation in 3% O<sub>2</sub> was used to measure the saturation coverages of organics because some decomposition intermediates that form during TPD did not leave the surface by 725 K, when heating was stopped. All the carbon-containing species desorbed, decomposed, or were oxidized to CO<sub>2</sub>, however, during TPO so that a more accurate measure of surface coverage was obtained. The saturation coverages, in μmol/g catalyst are: ethanol (280) acetaldehyde (330), acetic acid (410), and formic acid (355). A saturation coverage of formaldehyde was not measured due to difficulties in producing pure formaldehyde. The saturation coverage of ethanol, when normalized to the TiO<sub>2</sub> surface area of 50 m<sup>2</sup>/g, is 3.3 molecules/nm<sup>2</sup>, which agrees well with the value of 3.28 molecules/nm<sup>2</sup> measure by Kim *et al.* (19) using a microbalance.

**TABLE 1**  
**Amounts Desorbed during TPD and TPO ( $\mu\text{mol/g}$  Catalyst)**

Adsorbed molecule	Amount desorbed during TPD ( $\mu\text{mol/g}$ catalyst)								TPO (CO <sub>2</sub> )	Total <sup>a</sup> carbon
	Ethanol	C <sub>2</sub> H <sub>4</sub>	CH <sub>3</sub> CHO	CH <sub>3</sub> COOH	Acetone	HCOOH	CO	CO <sub>2</sub>		
Ethanol	165	77	42				22		35	625
Acetaldehyde			12				12	10	537	582
Acetic acid				92	123		53	141	84	831
Formaldehyde <sup>b</sup>							43		—	43
Formic acid						37	284	24	0	345

<sup>a</sup> Total carbon is the sum of the TPD and the TPO experiments.

<sup>b</sup> Not at saturation coverage.

Table 1 shows the amounts of desorption products detected during TPD to 723 K and during a subsequent TPO. These saturation coverages of ethanol, acetaldehyde, acetic acid, and formic acid are similar to those measured by TPO. During TPD of ethanol, approximately 60% of the ethanol desorbed in two broad peaks at 450 and 650 K (Fig. 1). The remaining ethanol either dehydrated to ethylene in a peak at 660 K, dehydrogenated to acetaldehyde at 650 K, or decomposed to CO in a peak at 660 K. The dehydration pathway was favored over the dehydrogenation pathway by a ratio of 1.8 to 1. Approximately 5% of the adsorbed ethanol remained on the catalyst surface in some form after TPD and was oxidized during the subsequent TPO.

During ethanol TPD on the {011}-faceted TiO<sub>2</sub> (001) surface, Kim and Barteau (20) detected ethanol, acetaldehyde, and ethylene at similar temperatures. However, they observed less dehydrogenation to acetaldehyde and did not detect any CO. On anatase powder, Kim *et al.* (19) reported that 61.8% of the ethanol desorbed, and acetaldehyde (9.4%), ethylene (8.8%), diethyl ether (6.5%), and water (4.7%) were detected along with other minor products.

In contrast to ethanol, acetaldehyde and its decomposition products were sufficiently strongly bound to the surface that less than 10% of the monolayer formed gas phase products during TPD, and the species remaining on the surface turned the catalyst brown at 723 K. During the subsequent TPO, these species were oxidized to CO<sub>2</sub>, and the total amount of carbon listed in Table 1 is less than observed during TPO of acetaldehyde. The TPD spectra in Fig. 2 shows that acetaldehyde desorbed with a maximum at 400 K and a shoulder at 655 K. High temperature CO and CO<sub>2</sub> were detected and their desorptions were incomplete when heating was stopped at 723 K. A small crotonaldehyde desorption peak near 400 K was observed but is not shown. An unidentified peak was observed during TPD of acetaldehyde, however, and this is at least partially responsible for the smaller amount of total carbon in Table 1 (582  $\mu\text{mol/g}$  catalyst) than observed during TPO only of a saturated surface (660  $\mu\text{mol/g}$  catalyst). Idriss and Barteau (21) investigated the selectivity and mechanism shifts during acetaldehyde TPD on TiO<sub>2</sub> (001). They observed the main reaction pathway changed from reductive coupling to aldol condensation as the surface was oxidized by annealing. For the

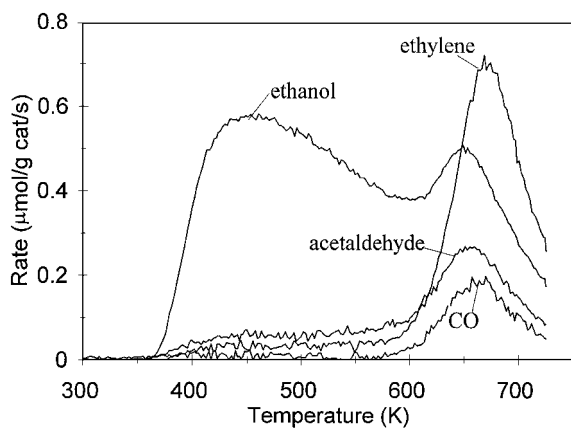


**FIG. 1.** Temperature-programmed desorption spectra of a monolayer of ethanol on TiO<sub>2</sub>.

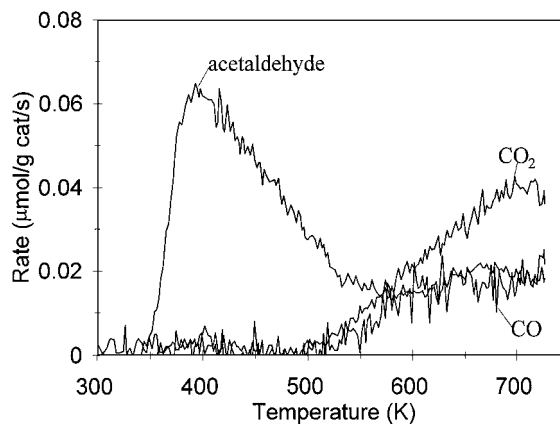


**FIG. 2.** Temperature-programmed desorption spectra of a monolayer of acetaldehyde on TiO<sub>2</sub>.

TiO<sub>2</sub> (001) surface annealed at 750 K, the TPD products were: acetaldehyde (30%), ethanol (36%), butene (1%), crotonaldehyde (19%), and crotyl alcohol (14%). Although we checked for all these products, no ethanol or butene and only small amounts of crotonaldehyde were detected. In addition, the TPO performed after TPD clearly indicates that acetaldehyde mainly decomposes to a stable species that does not desorb during TPD.

Acetic acid, acetone, CO, and CO<sub>2</sub> were the products detected during TPD of acetic acid (Fig. 3). Much of the acetic acid was strongly bound to TiO<sub>2</sub>, but approximately 22% desorbed. At high temperatures, 59% of the acetic acid reacted via bimolecular ketonization to form acetone. Carbon dioxide also formed at high temperature, as did CO. Much of the CO<sub>2</sub> is probably a product from the bimolecular ketonization. In addition, a small amount of CO formed at high temperature. The remaining 10% of the original carbon was oxidized to CO<sub>2</sub> during the subsequent TPO. A TPD study by Kim and Barteau (22) on anatase TiO<sub>2</sub> powder identified the same major TPD products, but with different yields: acetic acid (38%), CO<sub>2</sub> (28%), acetone (20%). In addition, Kim and Barteau detected significantly less CO (2%) and also observed ketene (11%) as a decomposition product. Since the appearance of acetone during TPD is a measure of surface acetic acid, its desorption rate is combined with that for acetic acid in most subsequent figures for clarity.

When a low coverage of formaldehyde decomposed during TPD, the only product detected was CO, which formed in a peak centered at 610 K. Henderson (23) reported that during TPD of formaldehyde on TiO<sub>2</sub> (110), the CO signal was an order of magnitude greater than those of formaldehyde, formic acid, and CO<sub>2</sub>. On an Ar<sup>+</sup>-bombarded TiO<sub>2</sub> (001) surface, formaldehyde, methanol, CO, and CO<sub>2</sub> were detected when TPD of formaldehyde was carried out (24). Only formaldehyde and methanol were observed on surfaces annealed above 700 K.

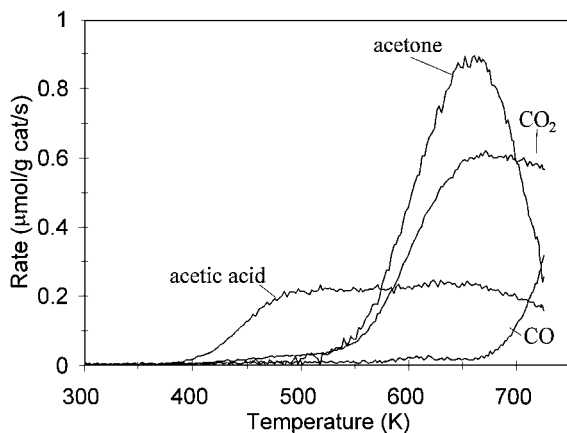


FIG. 3. Temperature-programmed desorption spectra of a monolayer of acetic acid on TiO<sub>2</sub>.

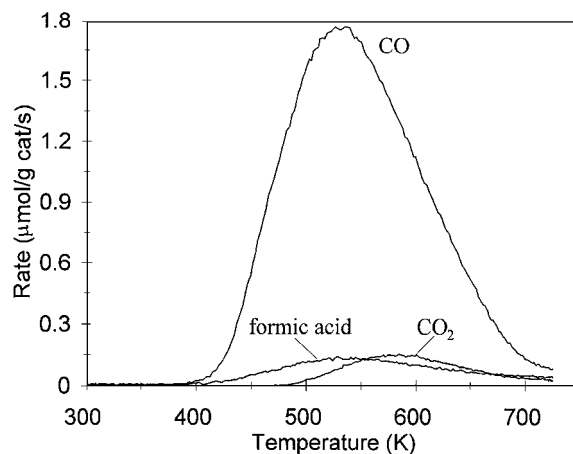


FIG. 4. Temperature-programmed desorption spectra of a monolayer of formic acid on TiO<sub>2</sub>.

Similar to formaldehyde, the main carbon-containing product from formic acid TPD was CO (82%), and smaller amounts of formic acid (11%) and CO<sub>2</sub> (7%) desorbed, as shown in Fig. 4. The formic acid desorbed in a broad peak and dehydrated to CO and H<sub>2</sub>O in a broad peak that had a maximum at 525 K. The subsequent TPO indicated that no carbon-containing species were present after TPD. The main carbon-containing product from TPD of formic acid on several single-crystal surfaces is also CO, with a peak temperature near 560 K (23, 25, 26). Kim and Barteau (25) reported that 50% of adsorbed formic acid decomposed to CO, 32% desorbed intact, and 18% formed CO<sub>2</sub> on a TiO<sub>2</sub> (001) surface. A similar product distribution (44% CO, 26% formic acid, 21% CO<sub>2</sub>, and 10% formaldehyde) was observed for a {114}-faceted TiO<sub>2</sub> (001) surface.

#### Temperature-Programmed Desorption of H<sub>2</sub>O, CO, and CO<sub>2</sub>

Neither CO nor CO<sub>2</sub> are strongly adsorbed on TiO<sub>2</sub>, and thus when the catalyst was exposed to either CO or CO<sub>2</sub> at room temperature, nothing desorbed during TPD. This means that when CO<sub>2</sub> forms as a product during PCO, it should immediately desorb, and thus the rate of appearance of CO<sub>2</sub> in the gas phase is an indication of the rate of a surface reaction. Similarly, when CO<sub>2</sub> forms during TPD or TPO, its rate of appearance in the gas phase is reaction limited. The presence of water on the surface may affect CO<sub>2</sub> adsorption, however, since we observed a small CO<sub>2</sub> desorption peak (3.5 μmol/g catalyst) with a maximum at 400 K during TPD for a water-saturated surface that was exposed to CO<sub>2</sub>. Since this CO<sub>2</sub> coverage is so low and since water coverage is not at saturation during PCO, the rate of appearance of CO<sub>2</sub> during PCO is expected to be limited by surface reaction.

In contrast, water readily adsorbed on TiO<sub>2</sub>, desorbed in a broad peak centered at 625 K, and continued to desorb

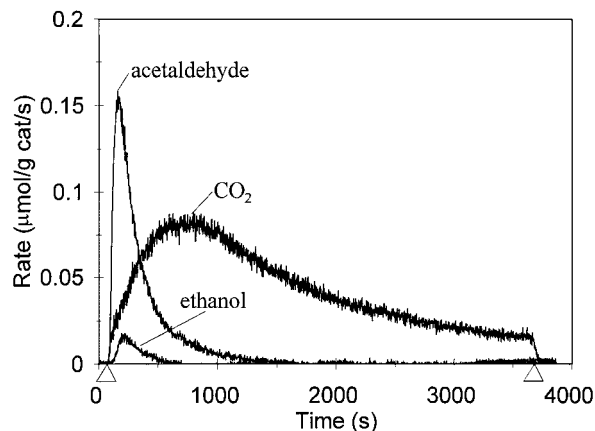


FIG. 5. Product desorption rates measured during PCO of a monolayer of ethanol on TiO<sub>2</sub> in 0.2% O<sub>2</sub>.

when the temperature ramp was stopped at 723 K. Saturation coverage corresponded to 750 μmol/g catalyst. Because water is strongly adsorbed on TiO<sub>2</sub>, its appearance in the gas phase does not provide kinetic information and thus for clarity the water signal is not presented in the TPD or PCO plots.

### Photocatalytic Oxidation of Ethanol

A monolayer of ethanol was oxidized photocatalytically for various reaction times (60–3600 s) in repeat experiments. As shown in Fig. 5, approximately 15% of the ethanol monolayer was rapidly oxidized photocatalytically to form gas-phase acetaldehyde. The remaining ethanol oxidized more slowly to CO<sub>2</sub> and H<sub>2</sub>O, and CO<sub>2</sub> production continued until the UV lights were turned off.

The species remaining on the surface were identified by TPD. Figure 6 shows the TPD spectra obtained after 1800 s of PCO of a monolayer of ethanol. Most of the ethanol

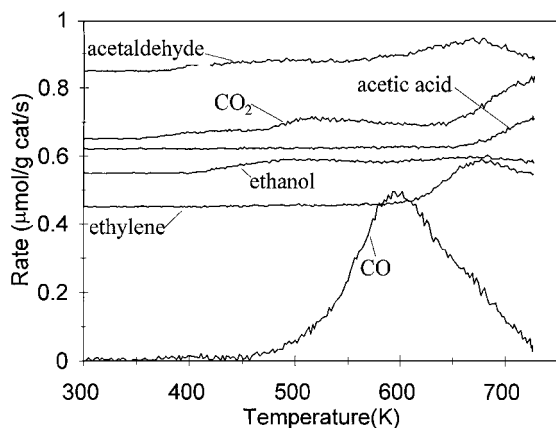


FIG. 6. Temperature-programmed desorption spectra of TiO<sub>2</sub> after 1800 s PCO of a monolayer of ethanol.

that did not oxidize during PCO either dehydrated to ethylene or dehydrogenated to acetaldehyde during TPD. Less than 3% of the original ethanol desorbed intact. Acetic acid started to desorb (and decompose to acetone) at 650 K and continued until heating was stopped at 723 K. The main species detected during TPD, however, was CO in a peak at 600 K; this CO is attributed to formaldehyde and formic acid decomposition. Since TPD of both formaldehyde and formic acid produce CO peaks near 600 K, resolving the contributions of each species to the CO peak is difficult. Carbon dioxide desorbed in a peak at 510 K and a second peak that had not reached a maximum when heating was stopped at 723 K. The low-temperature CO<sub>2</sub> peak is attributed to acetaldehyde and formic acid decomposition, since CO<sub>2</sub> started to form at 500 K during TPD of these species. The high-temperature CO<sub>2</sub> peak is attributed to decomposition of acetaldehyde and bimolecular ketonization of acetic acid.

Figures 7a and 7b show the amounts of products that desorb during TPD following different PCO times. The products that are attributed to desorption and decomposition

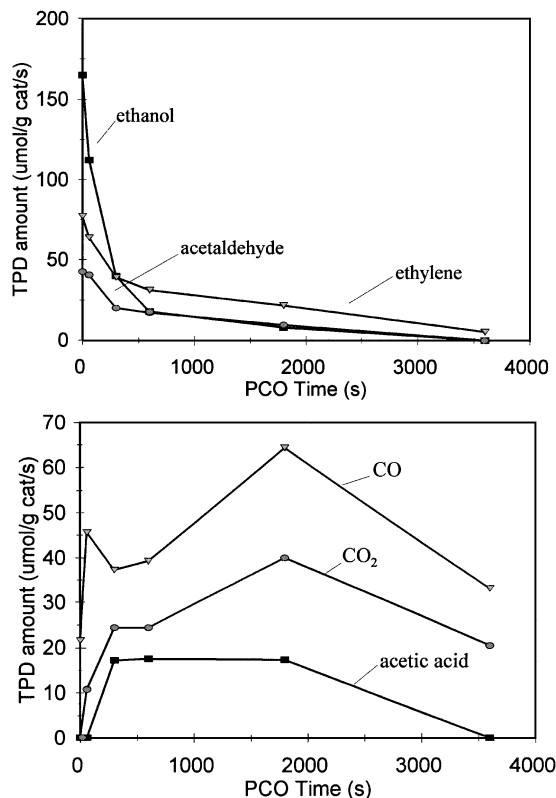


FIG. 7. Product desorption amounts measured during TPD after various PCO times of a monolayer of ethanol. (a) Ethylene and acetaldehyde are the respective dehydration and dehydrogenation products of ethanol present on the surface after PCO. (b) Carbon monoxide is the decomposition product of formaldehyde, formic acid, and at short reaction times, ethanol. Carbon dioxide is the decomposition product of formic acid, acetic acid, and acetaldehyde.

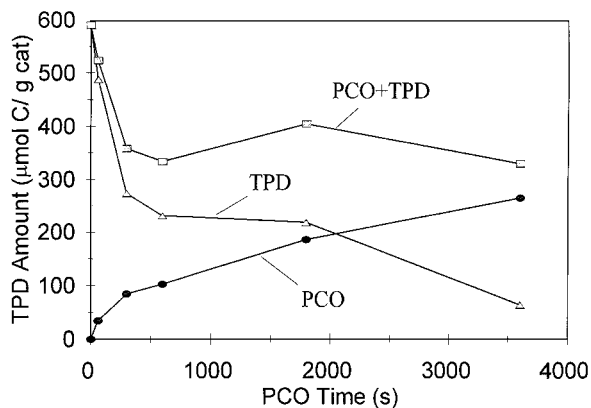


FIG. 8. Product desorption amounts measured during PCO and TPD after various PCO times of a monolayer of ethanol.

of unreacted ethanol are shown in Fig. 7a. The amount of ethanol that desorbed intact after PCO decreased with increasing PCO time more rapidly than the ethanol that dehydrogenated to acetaldehyde or dehydrated to ethylene. Figure 7b shows the amounts of intermediates on the surface. The amount of acetic acid on the surface was approximately constant up to 1800 s of PCO. The amount of CO, which is mostly due to formaldehyde and formic acid decomposition reached a maximum after 1800 s of PCO. Decomposition of unreacted ethanol also contributed to the CO, especially at shorter reaction times. The total amount of carbon in gas phase products from PCO plus TPD, as shown in Fig. 8, decreased from 590  $\mu\text{mol/g}$  catalyst before any PCO to 360  $\mu\text{mol/g}$  catalyst after PCO for 300 s, indicating that a strongly bound intermediate remained on the catalyst after TPD. After PCO (1800 s) and a TPD, a subsequent TPO oxidized this intermediate to 110  $\mu\text{mol CO}_2/\text{g}$  catalyst. The total amount of carbon detected during PCO, TPD, and TPO was 580  $\mu\text{mol/g}$  cat, which is close to the value obtained for saturation coverage of ethanol by TPO.

#### Photocatalytic Oxidation of $^{13}\text{C}$ -Labeled Ethanol

The PCO of a monolayer of ethanol, with the  $\alpha$ -carbon labeled with  $^{13}\text{C}$ , is shown in Fig. 9. Immediately after illumination, acetaldehyde (with  $^{13}\text{C}$  on the  $\alpha$ -carbon) and smaller amounts of ethanol (not shown) desorbed. Initially, the  $\alpha$ -carbon oxidized to  $^{13}\text{CO}_2$  faster than the  $\beta$ -carbon formed  $^{12}\text{CO}_2$ . The rate of  $^{13}\text{CO}_2$  formation reached a maximum after 600 s of illumination, whereas  $^{12}\text{CO}_2$  formation did not reach a maximum rate until after 1000 s. The  $^{13}\text{CO}_2$  and  $^{12}\text{CO}_2$  formation rates were equal after 1500 s of illumination and both quickly decreased to zero when the UV lights were switched off.

The TPD products (Fig. 10) after 1800 s of PCO of  $\text{CH}_3^{13}\text{CH}_2\text{OH}$  are the same as those observed for unlabeled ethanol. Interestingly, the amount of  $^{12}\text{CO}$  that desorbed was greater than the amount of  $^{13}\text{CO}$ . This indicates that

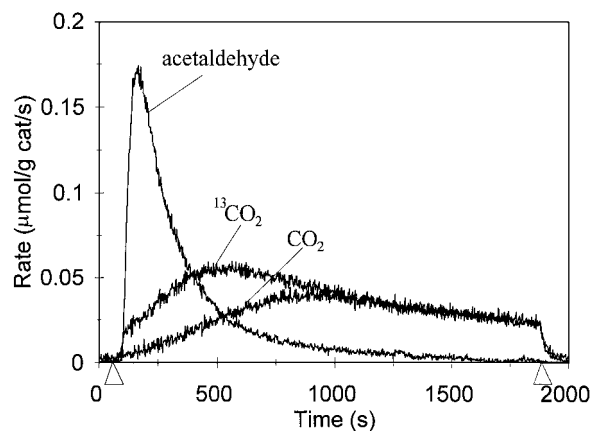


FIG. 9. Product desorption rates measured during PCO of a monolayer of  $^{13}\text{C}$ -ethanol on  $\text{TiO}_2$  in 0.2%  $\text{O}_2$ .

the majority of formic acid/formaldehyde on the surface after PCO came from the  $\beta$ -carbon. The total amount of  $^{12}\text{C}$  plus  $^{13}\text{C}$  for each species was similar to that for unlabeled ethanol. The total amount of carbon detected during PCO, TPD, and a subsequent TPO was 580  $\mu\text{mol/g}$  catalyst, which is close to the saturation coverage determined by ethanol TPO.

#### Photocatalytic Oxidation of Acetaldehyde

As shown in Fig. 11, during PCO, a monolayer of acetaldehyde oxidized to  $\text{CO}_2$  much slower than did ethanol. In contrast to ethanol, the  $\text{CO}_2$  rate reached a maximum almost as soon as the catalyst was exposed to UV and the rate decreased more slowly. Even though a monolayer of acetaldehyde contained more molecules than a monolayer of ethanol, the maximum  $\text{CO}_2$  rate was less than a third of the rate for ethanol PCO. Interestingly, the rate of  $\text{CO}_2$  formation was twice as high when the initial coverage

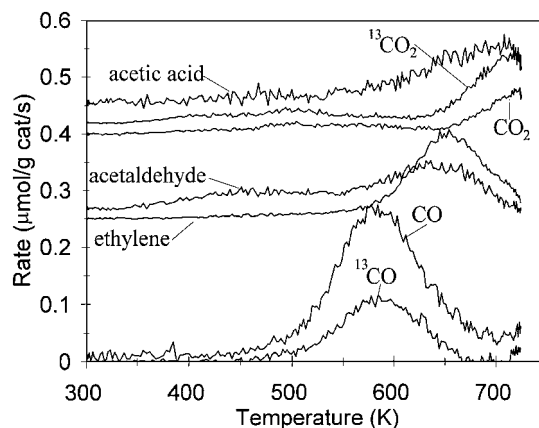


FIG. 10. Temperature-programmed desorption spectra of  $\text{TiO}_2$  after 1800 s PCO of a monolayer of  $^{13}\text{C}$ -ethanol.

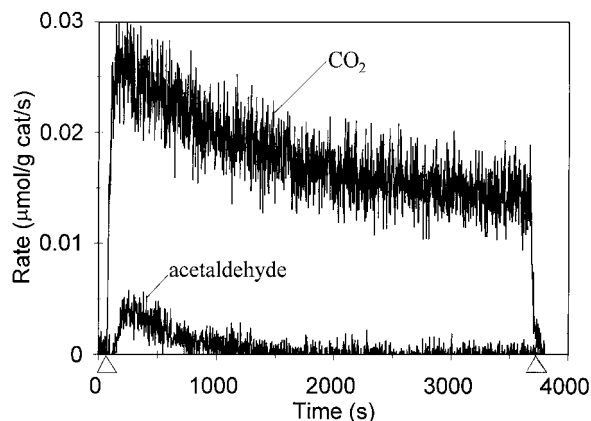


FIG. 11. Product desorption rates measured during PCO of a monolayer of acetaldehyde on TiO<sub>2</sub> in 0.2% O<sub>2</sub>.

of acetaldehyde was decreased. Moreover, the amount of acetaldehyde that desorbed during PCO was less than 5% of the amount that desorbed during PCO of a monolayer of ethanol.

In a series of experiments starting with a monolayer of acetaldehyde, TPD spectra were obtained after various PCO times, and the amounts detected during PCO and TPD are plotted in Fig. 12 versus the PCO time. In contrast to PCO of ethanol, for acetaldehyde the amount of carbon detected during PCO plus TPD *increased* with PCO time; for TPD a constant value of approximately 200 μmol/g catalyst was reached. That is, intermediates that were less strongly bound than acetaldehyde formed during PCO. More acetic acid desorbed during TPD after PCO than when ethanol was the reactant. Thus, after 3600 s of PCO, the total amount of organics that desorbed during TPD (Fig. 13) was greater for acetaldehyde than ethanol PCO, since the formic acid/formaldehyde amounts were similar. The acetaldehyde that did not react during PCO decomposed during TPD to form a stable surface species

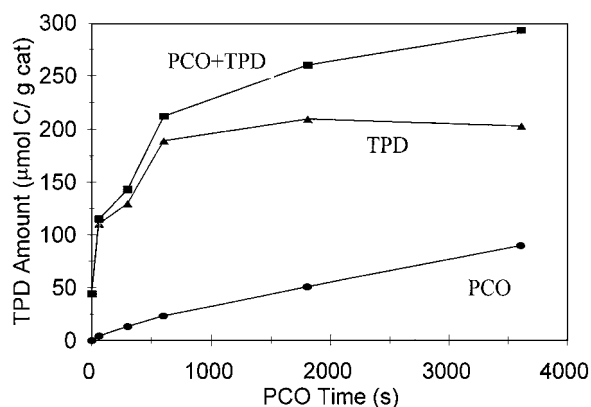


FIG. 12. Product desorption amounts measured during PCO and TPD after various PCO times of a monolayer of acetaldehyde.

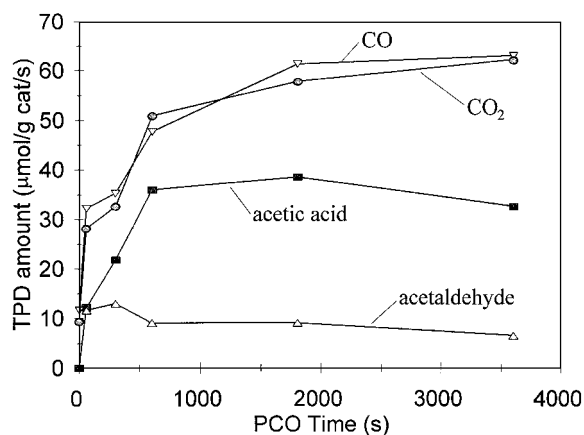


FIG. 13. Product desorption amounts measured during TPD after various PCO times of a monolayer of acetaldehyde.

that turned the catalyst brown. This surface species was oxidized to CO<sub>2</sub> and the catalyst was restored to its original state upon heating in oxygen at 723 K.

#### Photocatalytic Oxidation of <sup>13</sup>C-Labeled Acetaldehyde

As shown in Fig. 14 for PCO of a submonolayer coverage of CH<sub>3</sub><sup>13</sup>CHO, the α-carbon of acetaldehyde oxidized to <sup>13</sup>CO<sub>2</sub> faster than the β-carbon formed <sup>12</sup>CO<sub>2</sub>. Note that the rate of <sup>12</sup>CO<sub>2</sub> formation is almost constant after 250 s, and no acetaldehyde desorbed. The subsequent TPD spectra are similar to those obtained following PCO of <sup>13</sup>C-ethanol. The <sup>12</sup>CO desorbed at a higher rate than <sup>13</sup>CO, indicating that more adsorbed formic acid/formaldehyde was labeled with <sup>12</sup>C. The <sup>12</sup>C/<sup>13</sup>C ratio is smaller than obtained for TPD following ethanol PCO, but the initial coverages were different in the two experiments. A small ethylene peak was seen from decomposition of ethanol that was co-adsorbed on the surface from the <sup>13</sup>C-acetaldehyde generation process. The

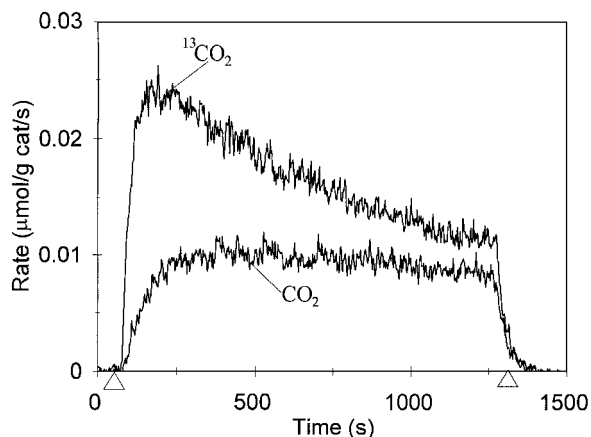


FIG. 14. Product desorption rates measured during PCO of a submonolayer of <sup>13</sup>C-acetaldehyde on TiO<sub>2</sub> in 0.2% O<sub>2</sub>.



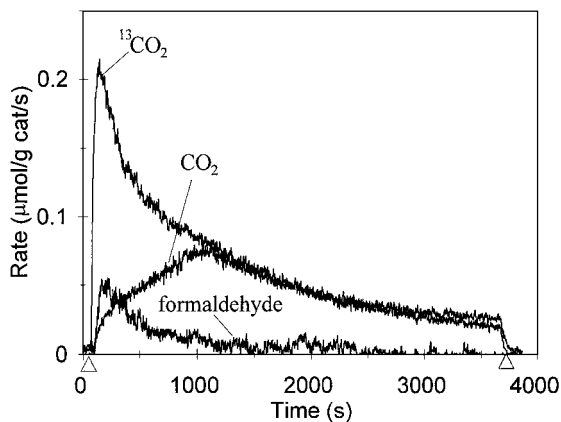


FIG. 15. Product desorption rates measured during PCO of a monolayer of  $^{13}\text{C}$ -labeled acetic acid on  $\text{TiO}_2$  in 0.2%  $\text{O}_2$ .

ethylene peak corresponded to an ethanol coverage that was approximately 5% of the acetaldehyde coverage.

#### Photocatalytic Oxidation of $^{13}\text{C}$ -Labeled Acetic Acid

During PCO of a monolayer of  $\text{CH}_3^{13}\text{COOH}$ ,  $^{13}\text{CO}_2$  formation rapidly reached a maximum rate after the catalyst was exposed to UV irradiation, whereas the rate of  $^{12}\text{CO}_2$  formation increased slowly to a maximum after 1050 s of illumination, as shown in Fig. 15. That is, the  $\alpha$ -carbon in acetic acid preferentially oxidized to  $\text{CO}_2$ , and only at long times were their rates comparable, and eventually the  $^{12}\text{CO}_2$  rate was higher. The rate of  $^{12}\text{C}$ -formaldehyde desorption, which is shown with arbitrary units due to calibration difficulties, quickly reached a maximum rate after the UV lights were turned on. For a lower coverage of  $\text{CH}_3^{13}\text{COOH}$ , no formaldehyde was detected in the gas phase and the rate of  $^{13}\text{CO}_2$  formation quickly reached a maximum during PCO (Fig. 16), whereas the  $^{12}\text{CO}_2$  rate reached a maximum after 850 s and was higher than the  $^{13}\text{CO}_2$  rate.

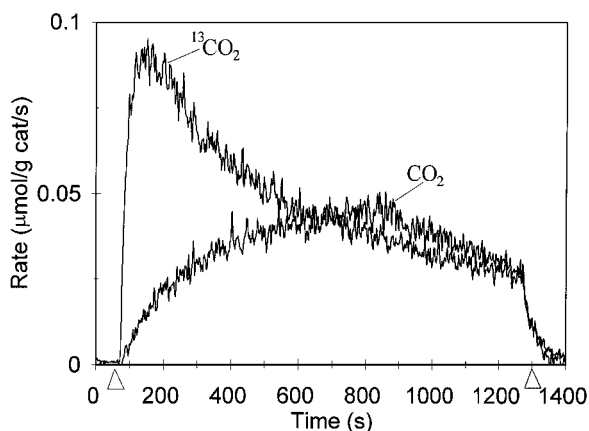


FIG. 16. Carbon dioxide desorption rates measured during PCO of a submonolayer of  $^{13}\text{C}$ -labeled acetic acid on  $\text{TiO}_2$  in 0.2%  $\text{O}_2$ .

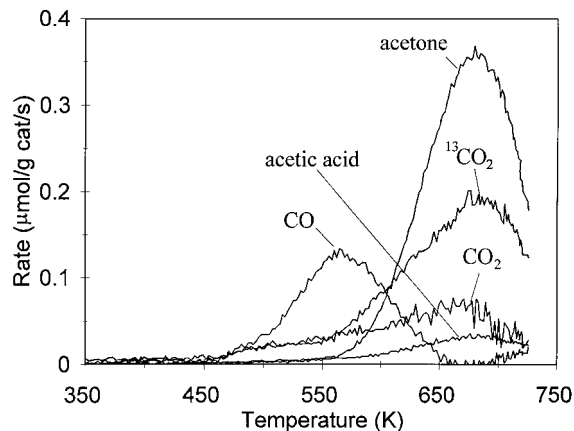


FIG. 17. Temperature-programmed desorption spectra of  $\text{TiO}_2$  after 3600 s PCO of a monolayer of  $^{13}\text{C}$ -labeled acetic acid.

The TPD spectra in Fig. 17 were obtained after the PCO in Fig. 15. Acetic acid, acetone,  $\text{CO}_2$ , and  $^{13}\text{CO}_2$  were observed and  $^{12}\text{CO}$  formed from decomposition of  $^{12}\text{C}$ -formaldehyde/formic acid. Acetone ( $\text{CH}_3^{13}\text{COCH}_3$ ),  $\text{CO}_2$ , and  $^{13}\text{CO}_2$  peaks at 680 K are attributed to bimolecular ketonization of acetic acid as reported by Kim and Barteau (22). Note that the acetone contained only one  $^{13}\text{C}$  atom, as would be expected for reaction between two acetic acid molecules to form acetone,  $^{13}\text{CO}_2$ , and  $\text{H}_2\text{O}$ . Thus, much more  $^{13}\text{CO}_2$  formed than  $^{12}\text{CO}_2$ . *No  $^{13}\text{CO}$  was observed in the TPD spectra.* Similar spectra were observed after 900 and 1800 s of PCO at saturation coverage. The absence of  $^{13}\text{C}$ -formaldehyde/formic acid indicates that the  $\alpha$ -carbon in acetic acid oxidized to  $^{13}\text{CO}_2$  without forming a stable intermediate. In contrast, the  $\beta$ -carbon formed  $^{12}\text{C}$ -formaldehyde/formic acid and some of it desorbed during PCO.

#### Photocatalytic Oxidation of Formaldehyde

During PCO of a low coverage of formaldehyde, the rate of  $\text{CO}_2$  formation was a maximum after 350 s of illumination (Fig. 18a); this delay indicated that formaldehyde oxidized through an intermediate, presumably formic acid. No other products were detected. During the subsequent TPD, only  $\text{CO}$  desorbed, and its peak temperature corresponded to either formaldehyde or formic acid decomposition. Since PCO of formaldehyde proceeds through a reaction intermediate, and the TPD after PCO shows that formic acid could be on the surface but no other species was detected, the intermediate is most likely formic acid.

#### Photocatalytic Oxidation of Formic Acid

During PCO of a monolayer of formic acid, the rate of  $\text{CO}_2$  formation quickly reached a maximum after UV illumination (Fig. 18b). This suggests either that formic acid oxidizes to  $\text{CO}_2$  in a single step, without proceeding

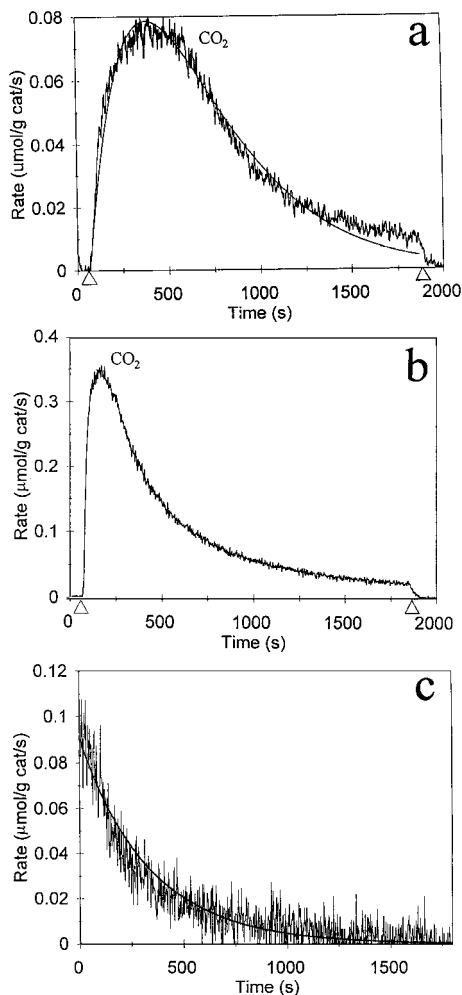


FIG. 18. (a) Carbon dioxide desorption rate measured during PCO of a submonolayer of formaldehyde on TiO<sub>2</sub> in 0.2% O<sub>2</sub> and a model fit. (b) Carbon dioxide desorption rate measured during PCO of a monolayer of formic acid on TiO<sub>2</sub> in 0.2% O<sub>2</sub>. (c) Model fit of the CO<sub>2</sub> decay curve during PCO of a submonolayer of formic acid on TiO<sub>2</sub> in 0.2% O<sub>2</sub>.

through long-lived reaction intermediates, or the reaction intermediates are much more reactive than formic acid. During the TPD after PCO, CO desorbed in a peak centered at 600 K, corresponding to formic acid decomposition. A small amount of formic acid also desorbed.

#### Kinetic Model of Reaction Steps

As discussed above, formaldehyde and formic acid decompose over the same temperature range to form CO so we cannot distinguish which of the two species is on the surface from the TPD spectra. The PCO rates for CO<sub>2</sub> formation can be used, however, to *estimate* rate constants if first-order surface reactions are assumed and the surface oxygen concentration is assumed constant. The series reaction was fit with two rate constants:



Since the PCO rate of formic acid to form CO<sub>2</sub> quickly reached a maximum and then decreased, the decreasing part of the curve for a submonolayer of formic acid was fit to an exponential, as shown in Fig. 18c. A low coverage of formic acid was used because only low coverages of formaldehyde could be readily obtained. The first-order rate constant  $k_2$  was  $3.0 \times 10^{-3} \text{ s}^{-1}$ , and this value was used to fit the 2-step reaction to the CO<sub>2</sub> curve from formaldehyde PCO and determine  $k_1$ . As shown in Fig. 18a, a good fit was obtained for  $k_1 = 3.3 \times 10^{-3} \text{ s}^{-1}$ . Since these rate constants are essentially the same, both formaldehyde and formic acid are expected to be on the surface during PCO of formaldehyde. Thus, PCO of formaldehyde has a time delay before the maximum rate of CO<sub>2</sub> production is reached because it is oxidizing through a formic acid intermediate. Essentially no delay is seen for formic acid PCO because no intermediate with a significant lifetime is present. Note that these rate constants were measured in the absence of gas-phase water, although Nimlos *et al.* (17) also reported values for the rate constants of formaldehyde and formic acid oxidation that were within 12% of each other (uncertainty of approximately 10% reported for formic acid rate-constant and not available for formaldehyde but they considered the uncertainty to be high).

## DISCUSSION

### Reaction Mechanism

The proposed reaction mechanism in Fig. 19 is based on our PCO, TPD, and TPO experiments and on previous studies. Almost immediately upon UV illumination, a portion of the adsorbed ethanol forms acetaldehyde, some

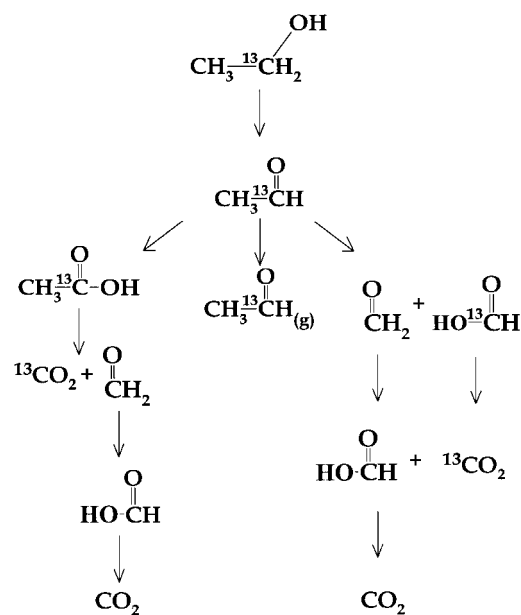


FIG. 19. Mechanism of the photocatalytic oxidation of ethanol.

of which desorbs at room temperature. The ethanol oxidizes to acetaldehyde on at least two types of sites; on one site acetaldehyde readily desorbs, whereas ethanol forms strongly bound acetaldehyde on the other site. Apparently gas-phase acetaldehyde adsorbs onto the latter type of site but not the former (27). The acetaldehyde that remains on the surface reacts by two parallel pathways to form either acetic acid or a formic acid/formaldehyde mixture. The  $\alpha$ -carbon of acetic acid then oxidizes to  $\text{CO}_2$  without forming a stable intermediate, whereas the  $\beta$ -carbon oxidizes to  $\text{CO}_2$  through formaldehyde and formic acid intermediates. Similarly, the formaldehyde produced directly from acetaldehyde subsequently oxidizes to  $\text{CO}_2$  through a formic acid intermediate. To be consistent with previous studies, we refer to the surface intermediates as formic acid and acetic acid, but they may be adsorbed as formate and acetate, since the acids are expected to dissociate on the  $\text{TiO}_2$  surface. The relative rates and the justifications for each of the steps in the proposed mechanism are presented below. Approximately 15% of the adsorbed ethanol ends up in the gas phase as acetaldehyde, 25% reacts through acetic acid, and the balance oxidizes directly through formic acid and formaldehyde (without the acetic acid intermediate). These percentages are for 0.2%  $\text{O}_2$  and a dry gas stream. When PCO was carried out in 20%  $\text{O}_2$ , the same behavior was observed as seen in 0.2%  $\text{O}_2$  (28). Similar behavior was also observed in the presence of water. Thus, the reaction mechanism appears to be the same during PCO in humid air, but the percentage of ethanol that follows each pathway depend on the water and  $\text{O}_2$  concentrations.

*Ethanol*  $\rightarrow$  *acetaldehyde*. The first step in PCO is ethanol oxidation to acetaldehyde. A portion of adsorbed ethanol could perhaps react through another intermediate, but the surface species detected by TPD after PCO of ethanol and acetaldehyde are the same. In addition, the surface compositions during PCO are remarkably similar for both until longer reaction times, when the lower coverage for ethanol decreases the amounts of TPD products detected.

A substantial amount of acetaldehyde desorbs almost immediately after UV illumination of an ethanol-covered surface (Fig. 5), indicating that ethanol quickly oxidizes to acetaldehyde without forming a stable intermediate. Some acetaldehyde desorbs presumably because it is displaced by water produced during PCO; as shown previously (1), a fraction of adsorbed acetaldehyde can be displaced by water. Since the surface is saturated and one molecule of ethanol makes two molecules (acetaldehyde and water) upon oxidation, some of the acetaldehyde may not have any adsorption sites available. However, much more acetaldehyde desorbs during PCO of a monolayer of ethanol than of a monolayer of acetaldehyde. Even when  $^{13}\text{C}$ -ethanol and acetaldehyde are co-adsorbed, approximately 90% of the acetaldehyde that appears in the gas phase is from ethanol (27). Thus, acetaldehyde probably appears in the gas phase

both because the surface is saturated and acetaldehyde adsorbs on different sites from ethanol.

Since ethanol reacts through an acetaldehyde intermediate, it is surprising that the rate of  $\text{CO}_2$  formation during PCO of a monolayer of acetaldehyde (Fig. 11) is lower than that for ethanol (Fig. 5). The acetaldehyde monolayer coverage is higher than that for ethanol, and during PCO of ethanol, 45 to 50  $\mu\text{mol/g}$  catalyst of acetaldehyde desorbs immediately, reducing surface coverage. In contrast, during acetaldehyde PCO, approximately one-tenth of this amount of acetaldehyde desorbs. Thus, the coverage of acetaldehyde is expected to be much higher when acetaldehyde was adsorbed from the gas phase than when ethanol was the adsorbate. However, PCO of half-saturation coverage of acetaldehyde formed  $\text{CO}_2$  twice as fast as a monolayer of acetaldehyde, and thus the lower rate of  $\text{CO}_2$  formation for adsorbed acetaldehyde is at least partly due to its higher coverage.

The dependence of acetaldehyde oxidation rate on coverage may also explain the difference in the  $^{13}\text{CO}_2$  and  $^{12}\text{CO}_2$  rates for various ethanol coverages, as reported previously (1). For half-saturation coverage of  $^{13}\text{C}$ -ethanol, the rate of  $^{13}\text{CO}_2$  formation quickly reaches a maximum after UV illumination, and no acetaldehyde desorbs. As shown in Fig. 9, however, PCO of a monolayer of  $^{13}\text{C}$ -ethanol exhibits maximum rates of  $^{13}\text{CO}_2$  and  $^{12}\text{CO}_2$  that are delayed in time. As shown in Fig. 12, after 3600 s of PCO of acetaldehyde, the amounts of acetic acid and formaldehyde/formic acid are greater than that for ethanol PCO of the same duration (Fig. 7b), but the rate of  $\text{CO}_2$  formation is slightly lower. Clearly, the presence of acetaldehyde decreases the reactivities of other intermediates on the surface.

*Acetaldehyde*  $\rightarrow$  *acetic acid*. TPD spectra following PCO show that both ethanol and acetaldehyde (Figs. 7b and 13) produce acetic acid as a reaction intermediate. At least one-fourth of a monolayer of ethanol reacted through an acetic acid intermediate. This was calculated by adding the amount of acetic acid on the surface to the difference in the amounts of  $^{13}\text{CO}$  and  $^{12}\text{CO}$  during TPD (Fig. 10). This difference after 1800 s of PCO is about the same as the difference in the amounts of  $^{13}\text{CO}_2$  and  $^{12}\text{CO}_2$  formed during PCO. Since PCO of acetic acid also exhibits a large difference in the rates of  $^{13}\text{CO}_2$  and  $^{12}\text{CO}_2$  formation, and PCO of  $\alpha$ - $^{13}\text{C}$ -acetic acid does not deposit  $^{13}\text{C}$ -formic acid or formaldehyde, all the acetaldehyde or ethanol does not react through the acetic acid pathway. This pathway is not active at longer reaction times, because no acetic acid is on the surface after 3600 s of PCO of ethanol (Fig. 7b) even though some ethanol is still present. This suggests that the acetic acid pathway is more active than the direct PCO of acetaldehyde to formaldehyde. In previous studies, Nimlos *et al.* (17) identified small amounts of acetic acid in the gas phase during PCO of both ethanol and acetaldehyde. Sauer and Ollis (18) did not detect acetic acid during PCO of

ethanol, but included it in their mechanism because of a shortage in their carbon mass balance.

*Acetaldehyde* → *formic acid and formaldehyde*. The TPD spectra (Fig. 17) after PCO of <sup>13</sup>C-acetic acid shows that only <sup>12</sup>C-formic acid/formaldehyde intermediates are on the catalyst surface; acetic acid does not form any stable <sup>13</sup>C intermediates. In contrast, the TPD spectra (Fig. 10) after PCO of <sup>13</sup>C-ethanol and <sup>13</sup>C-acetaldehyde show that both <sup>12</sup>C and <sup>13</sup>C-formic acid/formaldehyde are on the surface, so ethanol and acetaldehyde must react through a second pathway that does not produce acetic acid. If this second pathway involves direct oxidation of the carbons of acetaldehyde to formaldehyde and formic acid, then both <sup>12</sup>C and <sup>13</sup>C-formic acid/formaldehyde would be present on the surface from this pathway. The fact that much more <sup>12</sup>C-formic acid/formaldehyde than the <sup>13</sup>C species are on the surface during PCO of both <sup>13</sup>C-ethanol and <sup>13</sup>C-acetaldehyde indicates that both pathways are initially active. In addition, the CO TPD peaks indicate that similar amounts of formic acid/formaldehyde are on the surface during PCO of unlabeled ethanol and acetaldehyde (Figs. 7b and 13). In contrast, much less formaldehyde/formic acid is on the surface after PCO of a monolayer of acetic acid. This further indicates that both ethanol and acetaldehyde react through another pathway that does not produce an acetic acid intermediate. To estimate the fraction of ethanol that follows this pathway, we assumed that a molecule of acetaldehyde reacted to form both formaldehyde and formic acid.

*Acetic acid* → *CO<sub>2</sub> + formaldehyde*. The maximum rate of <sup>13</sup>CO<sub>2</sub> formation from <sup>13</sup>C-acetic acid occurs immediately after UV illumination regardless of surface coverage (Figs. 15 and 16), and no <sup>13</sup>C-intermediate was detected on the surface during TPD. This suggests that the formation of <sup>13</sup>CO<sub>2</sub> is most likely a single-step process. The α-carbon in acetic acid could oxidize to CO<sub>2</sub> in a two-step process if one step is much faster than the other, but the intermediate could not be formaldehyde or formic acid since these would be detectable during TPD. Since <sup>12</sup>C-formaldehyde appears in the gas phase during PCO of a monolayer of <sup>13</sup>C-acetic acid, it is directly identified as an intermediate. Also, TPD after PCO of <sup>13</sup>C-acetic acid shows <sup>12</sup>CO desorption peak near 600 K, which is an indication of <sup>12</sup>C-formaldehyde/formic acid on the surface during PCO.

The rates of <sup>13</sup>CO<sub>2</sub> and <sup>12</sup>CO<sub>2</sub> formation become nearly identical at long reaction times for both a monolayer and partial monolayer of acetic acid, and at sufficiently long times, the <sup>12</sup>CO<sub>2</sub> rate is *larger* than the <sup>13</sup>CO<sub>2</sub> rate (Figs. 15 and 16). As the concentration of <sup>12</sup>C-formaldehyde/formic acid builds up on the surface and the concentration of acetic acid decreases, we would expect the <sup>12</sup>CO<sub>2</sub> rate to be greater. It is also possible that some acetic acid reacts through another pathway, but the intermediates for such a pathway were not detected.

*Formaldehyde* → *formic acid*. During PCO of formaldehyde, the time delay before the maximum rate of CO<sub>2</sub> formation is reached (Fig. 18a) clearly indicates that formaldehyde forms CO<sub>2</sub> through an intermediate. Only CO desorbed during TPD following PCO of formaldehyde. Because both formaldehyde and formic acid produce a similar CO peak during TPD and because no other intermediates were observed, the intermediate is most likely formic acid. Nimlos *et al.* (17) also concluded that formaldehyde reacts through a formic acid intermediate to form CO<sub>2</sub> because the rate of formaldehyde destruction was greater than the rate of CO<sub>2</sub> evolution. In addition, they directly identified formic acid in the gas phase by FTIR.

Figure 18a shows that the maximum rate of CO<sub>2</sub> production during PCO of formaldehyde occurs after approximately 350 s of illumination. If the β-carbons in ethanol, acetaldehyde, and acetic acid all react through a formaldehyde intermediate, as proposed, the <sup>12</sup>CO<sub>2</sub> formation rates in the isotope studies should reach maxima after 350 s. This is observed for ethanol and acetic acid, but the <sup>12</sup>CO<sub>2</sub> rate from acetaldehyde is constant after 250 s (Figs. 9, 14, and 15); however, the acetaldehyde rate also shows a negative dependence on coverage.

*Formic acid* → *CO<sub>2</sub>*. Formic acid did not appear in the gas phase during PCO or TPD. However, TPD of formic acid (Fig. 4) shows a broad CO<sub>2</sub> peak starting at 450 K. Temperature-programmed desorptions after PCO of ethanol and acetaldehyde show similar low-temperature CO<sub>2</sub> peaks. Since the TPD spectra of both formaldehyde and formic acid have large CO peaks centered near 600 K, TPD does not provide unique identification of these molecules. The immediate maximum in the rate of CO<sub>2</sub> formation during PCO of formic acid (Fig. 18b) suggests that formic acid oxidation is a single-step process. In addition, TPD spectra after PCO of formic acid show only formic acid is on the catalyst, indicating that formic acid oxidation does not form a stable reaction intermediate.

### Relative Reaction Rates

The immediate appearance of acetaldehyde in the gas phase during ethanol PCO indicates the reaction to form acetaldehyde is faster than its subsequent oxidation to CO<sub>2</sub>. As shown in Fig. 8, the total amount of carbon detected during PCO and TPD after various reaction times of ethanol decreases from 590 to 360 μmol/g catalyst after PCO for 300 s and then remain fairly constant. This indicates that a strongly bound species that does not desorb (or decompose to a product that desorbs) during TPD formed on the surface in the first 300 s of PCO. Presumably this intermediate is acetaldehyde, since it is the only one identified that does not produce a significant amount of gas-phase species during TPD, although ethanol and acetic acid also deposit some carbon on the surface during TPD. In contrast, PCO and subsequent TPD of acetaldehyde after various

reaction times (Fig. 12) shows that the amount of intermediates detected during TPD *increases* with reaction time because acetaldehyde is oxidized to intermediates that desorb from the surface. Acetaldehyde and ethanol both react through the same intermediates. Since the total amount of carbon-containing species detected increases with reaction time for acetaldehyde, but decreases for ethanol (and ethanol forms acetaldehyde as an intermediate), the "missing" carbon is most likely due to an acetaldehyde intermediate.

For both acetaldehyde and ethanol, the amount of carbon-containing species detected during TPD remains fairly constant (until the acetaldehyde is used up) at about 200  $\mu\text{mol/g}$  catalyst (Figs. 8 and 12). For ethanol, this TPD amount decreases after 3600 s of PCO, presumably because not much acetaldehyde remains on the surface. For acetaldehyde, the surface coverage is substantially greater after 3600 s of PCO, since less products form during PCO and initial acetaldehyde coverage is greater than for ethanol.

Comparing the rates of  $\text{CO}_2$  evolution for ethanol and each intermediate is not sufficient for determining a rate-limiting step. In contrast to adsorption from the gas phase, reaction intermediates may adsorb on different sites or preferentially on one type of site when they are produced by PCO. Figure 7a shows that the amount of adsorbed ethanol decreases with PCO time more rapidly than  $\text{CO}_2$  forms, indicating ethanol oxidation is not rate-limiting. Figure 13 shows that during PCO of acetaldehyde, the amounts of acetic acid and formaldehyde/formic acid on the surface remain fairly constant after 600 s of PCO. Since acetaldehyde produces acetic acid and formaldehyde/formic acid intermediates at approximately the same rate as they are oxidized, it is difficult to isolate the rate-limiting step. Temperature-programmed desorption after PCO of acetic acid indicates the surface is mostly composed of acetic acid. This suggests that some of the acetic acid oxidizes to  $^{13}\text{CO}_2$  and  $^{12}$ formaldehyde slower than the subsequent oxidations of formaldehyde to formic acid and eventually  $\text{CO}_2$ . Figure 7b shows that although ethanol is still on the surface at longer reaction times, the acetic acid pathway has reacted to completion. This indicates that this pathway is more reactive than direct oxidation of acetaldehyde to formaldehyde/formic acid.

Sauer and Ollis (18) proposed that both acetic acid and formic acid oxidize quickly. Although no gas-phase acids were detected, the authors proposed that acetic acid and formic acid desorbed from the illuminated portions of the catalyst in the monolith reactor and collected on the dark  $\text{TiO}_2$ . However, the species that accumulated on the dark  $\text{TiO}_2$  is more likely either acetaldehyde or formaldehyde. Water can displace acetaldehyde (1), and formaldehyde was observed in the gas phase during PCO of acetic acid. However, water can only displace a fraction of the acetaldehyde, so some acetaldehyde that adsorbs on dark  $\text{TiO}_2$  may re-

main on the surface. During TPD after PCO, formic acid does not desorb and acetic acid only desorbs at high temperatures, indicating that these species are strongly bound to the surface and are not likely to desorb during PCO. Nimlos *et al.* (17) detected only small amounts of acetic acid during PCO.

Nimlos *et al.* suggested that the rate-limiting step is acetaldehyde oxidation, since its rate of disappearance was the slowest. However, acetaldehyde makes strongly bound intermediates, so fewer adsorption sites are open to acetaldehyde as PCO continues. In contrast, ethanol produces acetaldehyde as an intermediate, some of which readily desorbs during PCO. Since ethanol is able to displace some of the acetaldehyde during PCO, more sites are open for adsorption, so the disappearance of ethanol could be faster.

## CONCLUSIONS

The intermediates of ethanol PCO have been identified directly as acetaldehyde, acetic acid (acetate), formaldehyde, and formic acid (formate). Acetaldehyde forms immediately upon UV illumination, and at high coverages, some acetaldehyde desorbs or is displaced by water (1). The acetaldehyde that remains reacts by parallel pathways to either acetic acid or a formaldehyde/formic acid mixture. The  $\alpha$ -carbon in acetic acid preferentially reacts to  $\text{CO}_2$  and deposits the  $\beta$ -carbon as surface formaldehyde. The second pathway oxidizes the  $\alpha$  and  $\beta$ -carbons in acetaldehyde to formaldehyde and formic acid, respectively. The subsequent PCO of formaldehyde to  $\text{CO}_2$  proceeds through an intermediate, presumably formic acid.

The presence of acetaldehyde on the surface decreases the reactivity of other intermediates; thus, increasing the rate of acetaldehyde oxidation might increase the overall rate of  $\text{CO}_2$  production. The intermediate composition is relatively constant during PCO of ethanol and acetaldehyde, suggesting that acetaldehyde forms these intermediates at the same rate as they are oxidized. Of the two pathways proposed in the mechanism, the one through acetic acid is faster.

The application of transient reaction techniques is ideally suited for the study of photocatalytic oxidation since the reaction occurs at room temperature. Temperature-programmed desorption yields the direct identification of strongly bound intermediates, which do not appear in the gas phase during PCO. In addition, isotopic labeling clearly illuminates reaction pathways that would otherwise be indistinguishable.

## ACKNOWLEDGMENTS

Acknowledgment is made to the Donors of the Petroleum Research Fund, administered by the American Chemical Society for the support of this work. We also thank Kenneth M. Benjamin for carrying out the experiments with labeled acetaldehyde.

## REFERENCES

1. Muggli, D. S., Larson, S. A., and Falconer, J. L., *J. Phys. Chem.* **100**, 15886 (1996).
2. Sampath, S., Uchida, H., and Yoneyama, H., *J. Catal.* **149**, 189 (1994).
3. Jacoby, W., Nimlos, M., and Blake, D., *Env. Sci. Technol.* **29**, 1223 (1995).
4. Pichat, P., Herrman, J. M., Disdier, J., and Mozzanega, M., *J. Phys. Chem.* **83**, 3122 (1979).
5. Raupp, G. B., and Junio, C. T., *App. Surf. Sci.* **72**, 321 (1993).
6. Sauer, M. L., and Ollis, D. F., *J. Catal.* **149**, 81 (1994).
7. Sopyan, I., Marasawa, S., Hashimoto, K., and Fujishima, A., *Chem. Lett.* **4**, 723 (1994).
8. Stafford, U., Gray, K. A., Kamat, P. V., and Varma, A., *Chem. Phys. Lett.* **205**, 55 (1993).
9. Wada, K., Yoshida, K., Takatani, T., and Watanabe, Y., *App. Catal. A* **99**, 21 (1993).
10. Ait-Ichou, I., Formenti, M., Pommier, B., and Teichner, S. J., *J. Catal.* **91**, 293 (1985).
11. Aupo, M., Aikawa, N., and Kubokawa, Y., *J. Phys. Chem.* **88**, 3998 (1984).
12. Jacoby, W., Blake, D., Noble, R. D., and Koval, C. A., *J. Catal.* **157**, 87 (1995).
13. Larson, S. A., Widegren, J. A., and Falconer, J. L., *J. Catal.* **157**, 611 (1995).
14. Djeghri, N., and Teichner, S. J., *J. Catal.* **62**, 99 (1980). *Technol.* **30**, 3102 (1996).
15. Blake, N. R., and Griffin, G. L., *J. Phys. Chem.* **92**, 5697 (1988).
16. Cunningham, J., Hodnett, B. K., and Walker, A., *Proc. Royal Irish Acad.*, 411 (1977).
17. Nimlos, M. R., Wolfrum, E. J., Brewer, M. L., Fennell, J. A., and Bintner, G., *Environ. Sci.*
18. Sauer, M. L., and Ollis, D. F., *J. Catal.* **158**, 570 (1996).
19. Kim, K. S., Barteau, M. A., and Farneth, W. E., *Langmuir* **4**, 533 (1988).
20. Kim, K. S., and Barteau, M. A., *J. Mol. Cat.* **63**, 103 (1990).
21. Idriss, H., and Barteau, M. A., *Catal. Lett.* **40**, 147 (1996).
22. Kim, K. S., and Barteau, M. A., *Langmuir* **4**, 945 (1988).
23. Henderson, M. A., *J. Phys. Chem.* **101**, 221 (1997).
24. Idriss, H., Kim, K. S., and Barteau, M. A., *Surf. Sci.* **262**, 113 (1992).
25. Kim, K. S., and Barteau, M. A., *Langmuir* **6**, 1485 (1990).
26. Henderson, M. A., *J. Phys. Chem.* **99**, 15253 (1995).
27. Muggli, D. S., and Falconer, J. L., *J. Catal.*, submitted.
28. Muggli, D. S., Lowery, K. H., and Falconer, J. L., in preparation.